Journal of Luminescence 176 (2016) 32–39

Contents lists available at ScienceDirect

Journal of Luminescence

journal homepage: www.elsevier.com/locate/jlumin

Full Length Article

Influence of the infrared stimulation on the optically stimulated luminescence in four K-feldspar samples

G. Kitis [a,*], G.S. Polymeris [b], E. Şahiner [a,b], N. Meriç [b], V. Pagonis [c]

[a] Aristotle University of Thessaloniki, Nuclear Physics Laboratory, 54124 Thessaloniki, Greece
[b] Institute of Nuclear Sciences, Ankara University, Beşevler 06100, Ankara, Turkey
[c] McDaniel College, Physics Department, Westminster, MD 21157, USA

ARTICLE INFO

Article history:
Received 6 October 2015
Received in revised form
24 November 2015
Accepted 15 February 2016
Available online 18 March 2016

Keywords:
Thermoluminescence
Optically stimulated luminescence
Infrared stimulated luminescence
Feldspars
Luminescence dating
Localized recombination

ABSTRACT

Many dating protocols involve combined measurements of thermoluminescence (TL), optically stimulated luminescence (OSL) and infrared stimulated luminescence (IRSL). Although the physics behind each stimulation mode is entirely different, it is possible that all of these stimulation modes act on the same set of electron trapping levels existing in dosimetric materials. Therefore, one might expect that the experimental results of the combined TL, OSL and IRSL measurements may be correlated. The present work deals with the correlation between IRSL and OSL signals. The experimental protocol involves an initial exposure of the irradiated sample to infrared radiation (IR) for various stimulation times, and then recording the continuous-wave OSL signal (CW-OSL) of the same sample. In this way one can follow how the exposure to IR influences the trapping levels responsible for the CW-OSL signal. The results of the experiments showed that the IR stimulation influences these trapping levels which are responsible for the fast components of the CW-OSL decay curve, and not the trapping levels responsible for the slow CW-OSL components. The IRSL decay curves are described by analytical equations derived from a localized tunneling recombination model. On the other hand, the CW-OSL decay curves were fitted successfully with either one of two following methods; Firstly they were fitted by using an analytical expression derived from the solution of the one trap one recombination center model (OTOR), which describes delocalized recombination processes. Secondly, the CW-OSL decay curves were also fitted successfully using the same analytical expressions used for fitting the IRSL decay curves, based on localized transition processes. A more detailed analysis of the CW-OSL signals for stimulation durations up to 100 s, showed that the description of the CW-OSL using the localized tunneling recombination expression is superior to the description which uses the delocalized OTOR model.

1. Introduction

The study of thermoluminescence (TL), optically stimulated luminescence (OSL) and infrared stimulated luminescence (IRSL) properties of feldspars is a major field of research in luminescence dating. Feldspars have very good dosimetric properties, and can in principle contribute to the dating of every site of archeological and geological interest. However, the generalization of their use in dating is prohibited by the anomalous loss of their TL and OSL signal after irradiation, which contradicts the predictions of the standard TL kinetic theory based on delocalized transitions. This anomalous signal loss is known as the anomalous fading (AF) effect, and is attributed to the quantum tunneling effect which involves localized transitions [1–3].

Luminescence dating protocols usually include combined TL, OSL and IRSL measurements. The physics behind any of these stimulated effects is entirely different. However, it is possible that all these stimulation modes access the same electron tapping levels where the radiation dose is stored. Therefore, this possible common origin of these signals is likely to introduce a correlation between the experimentally observed luminescence signals. Correlation studies between TL, OSL and IRSL signals can provide very useful information about the electron traps from which these signals originated. Once the common electron trapping levels are identified, the stability of these signals over time can be studied with confidence.

The above mentioned correlation studies require detailed analysis of the complex experimental TL, OSL and IRSL signals, by using a computerized component resolved analysis (CCRA). The CCRA requires an analytical expression describing each component. In the case of OSL, these expressions are commonly based on

* Corresponding author.
E-mail address: gkitis@auth.gr (G. Kitis).

http://dx.doi.org/10.1016/j.jlumin.2016.02.023
0022-2313/

the empirical general order kinetics [4], or on mixed order kinetics models [5].

The usual analytical expressions for both general order kinetics [4] and mixed order kinetics [5] are entirely empirical. In the present work we will use for the first time new analytical expressions, which were recently derived from the solution of the one trap one recombination center model (OTOR) [6].

In the case of IRSL signals, new analytical expressions for CCRA were recently derived by Kitis and Pagonis [7], based on the delocalized transition model of Jain et al. [8,9].

The aim of the present work is a correlation study between CW-IRSL and remnant CW-OSL signals in natural feldspar samples. More specifically, the goals of this work are:

- To investigate the influence of the IR stimulation on electron traps which are also responsible for the CW-OSL signal.
- To apply a CCRA on the CW-OSL decay curves using newly developed analytical expressions derived from the OTOR model, which are based on delocalized transitions [6].
- To apply a second CCRA method on the same CW-OSL decay curves, by using analytical expressions derived from the model by Jain et al. [9], involving localized transitions and tunneling processes.
- To apply the same CCRA method based on tunneling, to the experimental CW-IRSL decay curves .
- To compare the two methods of analysis of the CW-OSL and CW-IRSL curves, and to decide whether these signals are better described by localized or delocalized transition models.

2. Experimental procedure

2.1. Samples, apparatus and measurement conditions

The K-feldspar samples used in the present work were two sanidine samples (with laboratory reference bal2 and sam3 hereafter), one orthoclase sample (with laboratory reference vrs8) and one microcline sample (with laboratory reference kst4) [10,11]. Aliquots (sub-samples) with the same mass of 5 mg and grain dimensions between 80 and 150 μm were attached to stainless steel disks.

All luminescence measurements were carried out using a Risø TL/OSL reader (model TL/OSL-DA-20), equipped with a high power blue LED light source (470 nm, FWHM 20 nm), an infrared solid state laser (880 nm, FWHM 75 nm) and a $^{90}Sr/^{90}Y$ beta particle source, delivering a nominal dose rate of 0.1083 Gy/s. A 9635QA photomultiplier tube with a Hoya (U-340) blue filter were used for light detection (340 nm, FWHM 80 nm). All measurements were performed in a nitrogen atmosphere with a low constant heating rate of 2 °C/s, in order to avoid significant temperature lag, and the samples were heated up to the maximum to temperature of 500 °C. The OSL stimulation wavelength is 470 ± 20 nm for the case of blue stimulation, delivering at the sample position a maximum power of 40 mW/cm^2. For IRSL, the stimulation wavelength is 880 ± 75 nm and the maximum power 135 mW/cm^2.

2.2. Experimental protocol

The experimental procedure used is described by the following protocol:

- Step 1: Irradiation with a test dose of 40 Gy.
- Step 2: Continuous wave IRSL (CW-IRSL) at room temperature for time t_i.
- Step 3: CW-OSL at room temperature for 1000 s to obtain the residual OSL signals (ROSL). Hereafter, these CW-OSL curves will be referred as ROSL curves.
- Step 4: TL measurement up to a temperature $T=500$ °C at 2 °C/s to obtain the residual TL signal.
- Step 5: Repeat steps 1–4 for a new CW-IRSL stimulation time t_i in step 2.

The IR stimulation times used were $t_i=0$, 5, 10, 25, 35, 50, 75, 100, 250, 500 and 1000 s. The case of time $t_i=0$ corresponds to the CW-OSL signal with no prior IR stimulation.

The experimental protocol described above was applied on a single aliquot. This makes necessary sensitivity variation tests. The sensitivity test was performed by recording a TL glow-curve up to 500 °C for the test dose of 40 Gy, between steps 4 and 5, after the stimulation times 10, 50, 250 and 1000 s. The five TL glow-curves obtained from this procedure showed a reproducibility better that 2%. This result means that sensitivity corrections are not required.

3. General remarks

Fig. 1 shows the TL glow-curves of bal2 feldspar for a dose of 40 Gy and the residual TL signal remaining after the IRSL exposure in step 2, followed by 1000 s measurement of the CW-OSL in step 3 of the experimental protocol. In all cases the integrated residual TL signal is less than the 5% of the integrated TL glow-curve signal. The conclusion is that this double IRSL and CW-OSL stimulation causes an almost complete optical bleaching of the energy levels responsible for the entire TL glow-curve. Fig. 1 is representative for all feldspar samples in the present work.

Upper Fig. 2 shows examples of ROSL decay curves measured after the sample was exposed to IR stimulation for 0, 25, 100 and 1000 s. The other three feldspar samples exhibit the exact same behavior. It is clear that the IRSL stimulation (step 2) has a strong effect on the subsequently measured CW-OSL signal (step 3), up to a stimulation time between 100 and 200 s. For higher stimulation times there is no influence on the CW-OSL decay curves by the prior IRSL stimulation. The experimental data in Fig. 2 also provides a strong indication that the same trapping levels may be contributing to both IRSL and ROSL signals.

The CW-OSL curves are featureless curves. The lower Fig. 2 shows the Linearly modulated OSL (LM-OSL) curves for these

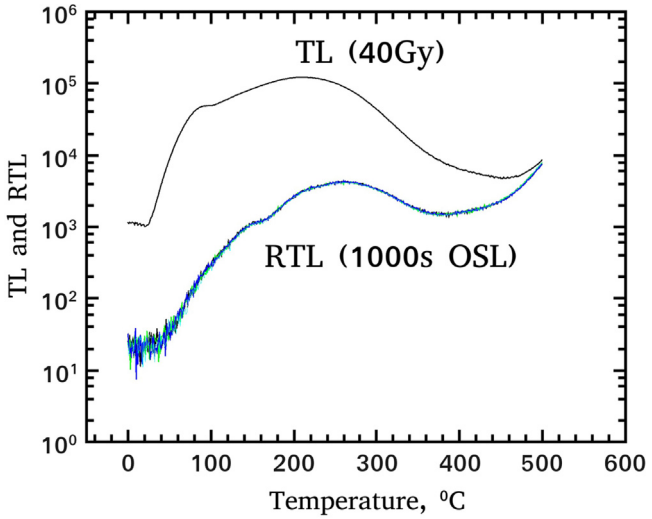

Fig. 1. TL signal of sample bal2 induced by 40 Gy of beta irradiation, and the residual TL glow-curves left after 0, 500 and 1000 s IR exposure (step 2 of the protocol), followed by a CW-OSL measurement of 1000 s (step 3 of the protocol).

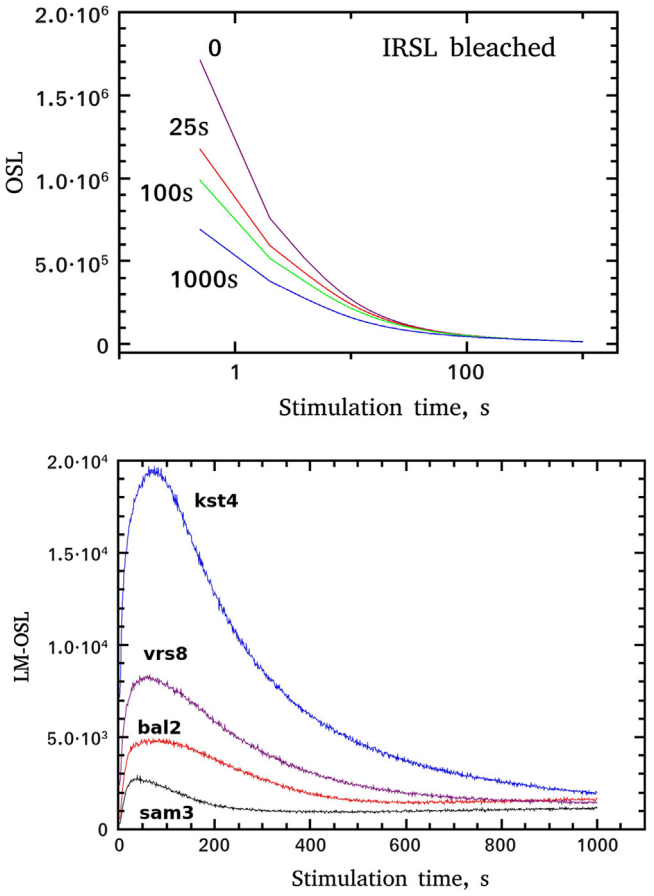

Fig. 2. Upper figure: residual CW-OSL decay curves (ROSL) for bal2 remaining after IR bleaching for 0 s (unbleached sample), 25 s, 100 s and 1000 s in step 2 of the protocol. Lower figure: LM-OSL curves for the four K-feldspar samples.

samples. The shape of these curves clearly shows that the OSL signal from the K-feldspars studied in this paper consists of more than one component.

Taking into account that the CW-IRSL signal is due to localized transitions, it is of interest to examine whether the ROSL signal in these materials can be attributed to delocalized or to localized transitions, as it was done by Sfampa et al. [11]. Therefore, the analysis of the ROSL decay curves shown in Fig. 2 will be attempted in this paper by using both delocalized and localized transition models. The methods of analysis are described in detail in the next sections.

4. Method of analysis

4.1. Analysis based on a delocalized transition model

The usual kinetic theories providing analytical expressions for analysis of complex CW-OSL decay curves are the empirical general order kinetics [4], as well as the mixed order kinetics [5]. In the present work we use new expressions derived from the solution of the one trap one recombination center model (OTOR). The OTOR model is the most fundamental model used in the TL and OSL literature. Kitis and Vlachos [6] solved the set of differential equations describing this model in analytical form by using the Lambert W function. For the case of CW-OSL the analytical expression given by Kitis and Vlachos [6] for the case of CW-OSL signals is

$$I(t) = \frac{C}{W(e^z) + W(e^z)^2}. \tag{1}$$

The parameter z is given by the following equation:

$$z = \frac{R}{1-R} - \ln\left(\frac{1-R}{R}\right) + \frac{A\,t}{1-R}, \tag{2}$$

where C is a constant related to the total concentration of traps N and the initial concentration of trapped electrons n_0. The constant R represents the ratio $R = A_n/A_m$ with A_n and A_m being the retrapping and recombination coefficients respectively (in $cm^3\ s^{-1}$), A is the optical stimulation probability (in s^{-1}) given by

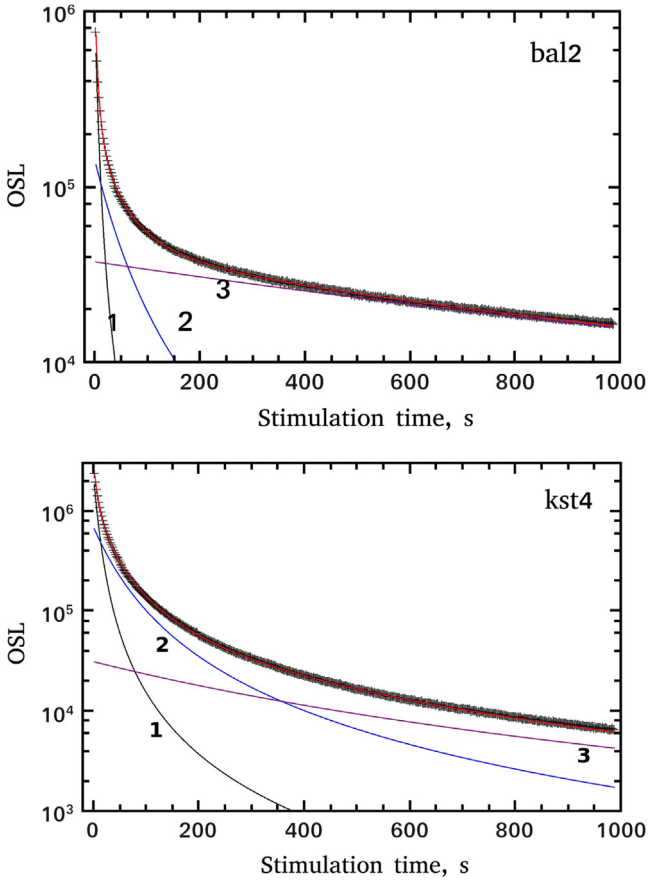

Fig. 3. ROSL decay curves for samples bal2 and kst4, after 0 s of IR stimulation (in step 2 of the protocol). These curves were analyzed using Eq. (1) derived from the solution of the OTOR model.

Table 1
Values of the parameter λ (in s^{-1}) and $R = A_n/A_m$ of each component from the fitting of the CW-OSL decay curves using Eq. (1) (see Fig. 3).

Sample	λ_1 (s^{-1})	λ_2 (s^{-1})	λ_3 (s^{-1})
bal2	0.157 ± 0.012	0.016 ± 0.003	$0.0006 \pm 4 \times 10^{-5}$
sam3	0.130 ± 0.011	0.013 ± 0.004	$0.0006 \pm 6 \times 10^{-5}$
vrs8	0.087 ± 0.004	0.016 ± 0.002	$0.0009 \pm 6 \times 10^{-5}$
kst4	0.091 ± 0.003	0.017 ± 0.002	$0.0018 \pm 4 \times 10^{-4}$
	R_1	R_2	R_3
bal2	0.43 ± 0.09	0.73 ± 0.09	0.78 ± 0.05
sam3	0.41 ± 0.07	0.74 ± 0.07	0.85 ± 0.02
vrs8	0.36 ± 0.03	0.64 ± 0.03	0.83 ± 0.04
kst4	0.41 ± 0.05	0.67 ± 0.02	0.77 ± 0.02

$A=\lambda=\sigma\cdot I_0$, with σ representing the IRSL or OSL cross section and I_0 the corresponding stimulation intensity.

The function $W(z)$ is the Lambert W function [12]. The parameter z given by Eq. (2) is very crucial for the application of the Lambert W function, due to the presence of the logarithmic term. In the present work we consider only the case of $R<1$, which corresponds to kinetic order b values between 1 and 2 in the empirical general order kinetics.

As discussed in detail by Kitis and Vlachos [6], Eq. (1) is a general equation holding for any stimulation mode: TL, CW-OSL, Linearly Modulated OSL etc. The superiority of using Eq. (1) for the case of TL, relative to the empirical general and mixed order kinetics equations, was shown in detail by Sadek et al. [13–16].

It must be noted that the application of Eq. (1) is somewhat complicated when one has to use analytical approximations for the Lambert function [6]. On the other hand, its application is very simple in software packages (for example MATHEMATICA, MATLAB) which contain the Lambert W function as a built-in function, just like other usual transcendental functions (sine, cosine etc.). In the present work the ROOT data Analysis Framework was used [17]. All fittings were performed using the MINUIT program [18] released in ROOT, which is a physics analysis tool for function minimization. The Lambert function W is implemented in ROOT through the GNU scientific library (GSL) [19].

4.2. Analysis based on a localized transition tunneling model

The ROSL and IRSL decay curves measured in the present work were also analyzed using the localized model of Jain et al. [9]. Specifically, three different published versions of this model are used, as follows.

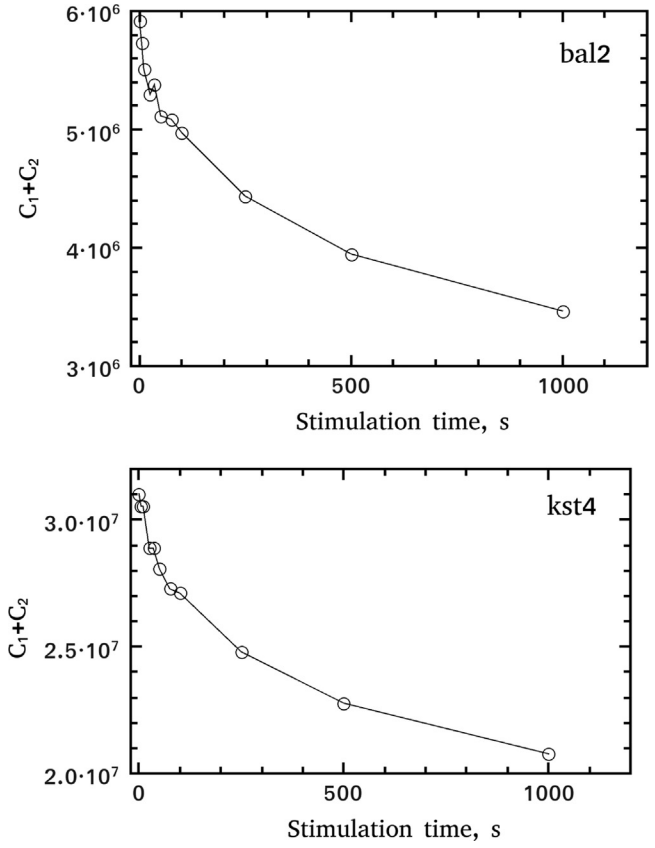

Fig. 4. The behavior of the sum of the two components (fast and medium) of the ROSL decay curves, as a function of the prior IR stimulation time, for samples bal2 and kst4. These curves were analyzed using Eq. (1) derived from the solution of the OTOR model.

Firstly, we use the analytical equations derived by Kitis and Pagonis [7]. These authors obtained analytical solutions of the set of differential equations in the model of Jain et al. [9], by using certain mathematical and physical simplifications. These authors presented analytical expressions describing several thermally and optically stimulated luminescence signals within this model. In the case of continuous wave optical simulation, the derived analytical expression is

$$I(t)=\frac{CF(t)^2}{f(t)}\cdot\exp\left(-\rho' F(t)^3\right) \tag{3}$$

$$F(t)=\ln(1+z\,A\,t) \tag{4}$$

$$f(t)=1+z\,A\,t \tag{5}$$

$$A=\lambda=\frac{1}{\tau} \tag{6}$$

where C is a constant proportional to the initial concentration of trapped electrons and ρ' is a dimensionless parameter representing the concentration of charge carriers. The quantity $A\ (s^{-1})$ represents the stimulation probability for the infrared or optical stimulation process, and can also be described by the characteristic time constant τ such that $A=\lambda=1/\tau$. In the above equation $z=1.8$ represents a constant in the model. It is noted that the above equations are used in this paper for comparison purposes on an empirical basis, and in principle they may not be applicable for analyzing OSL signals from samples which underwent a prior isothermal treatment or a prior optical bleaching.

Secondly, we use equations derived recently by Jain et al. [20]. These authors extended their localized transition model to include Arrhenius analysis and to develop equations applicable for

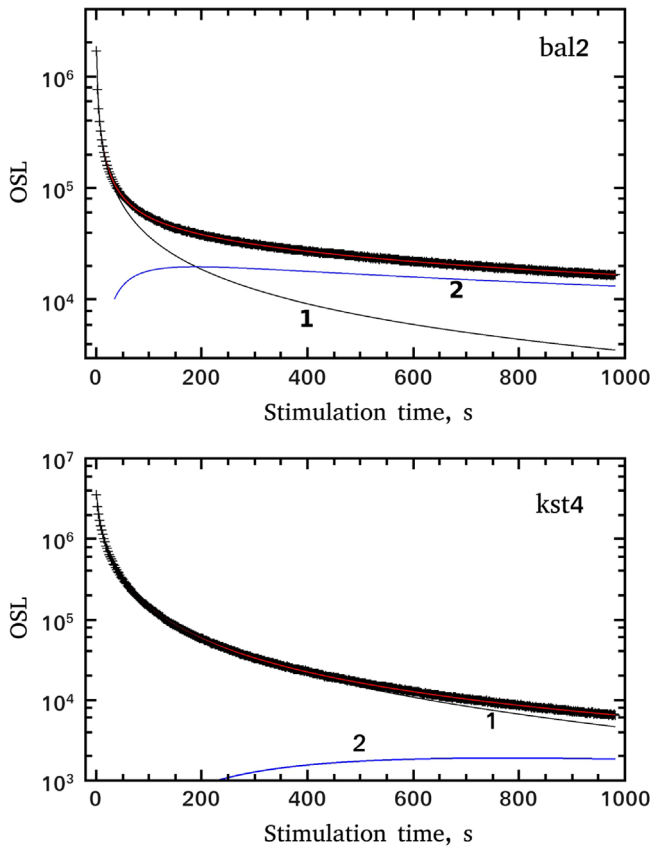

Fig. 5. ROSL decay curves for samples bal2 and kst4, after 0 s of prior IR stimulation time, analyzed using Eq. (3) derived from the solution of a localized tunneling recombination model.

truncated nearest neighbor distributions. Their model was used to describe successfully the behavior of IRSL signals from preheated feldspar samples, and was tested using experimental data. An important result of their extended model is that a prior isothermal or optical treatment of the samples results in a shifted time domain of the luminescence data.

The main equation derived by Jain et al. [20] is Eq. (3), but with the functions $F(t)$ and $f(t)$ given by

$$F(t) = \ln\left(J(\tau_0 + zt)\right) \tag{7}$$

$$f(t) = \tau_0 + zt \tag{8}$$

$$J = be^{-\xi} \tag{9}$$

where b is the attempt-to-tunneling frequency factor, τ_0 is a time shift constant, and $\xi = \ln(s/\sigma I_o)$ with s the frequency factor, σ is the optical cross-section and I_0 is the stimulation intensity.

Thirdly, we use equations derived recently by Pagonis et al. [21]. In a work similar to the extended model by Jain et al. [20], Pagonis et al. [21] presented new analytical equations to describe luminescence signals from samples which underwent prior thermal or optical treatments. The equations derived by Pagonis et al. [21] were compared with experimental data from a feldspar sample which underwent an isothermal procedure followed by measurement of the CW-IRSL signal. Additional comparisons with experiment were provided

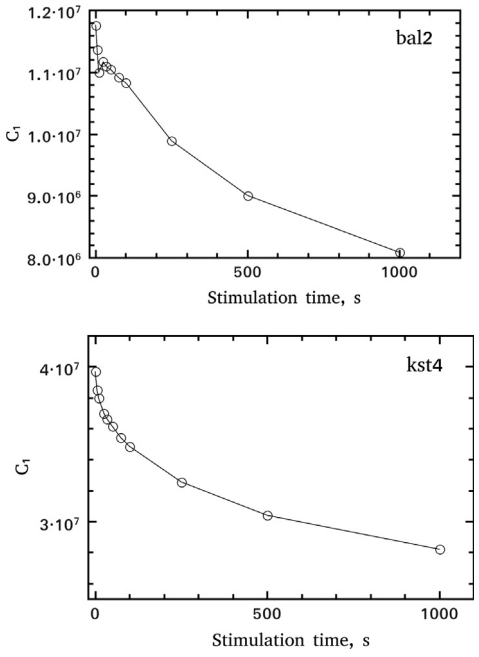

Fig. 6. The behavior of the fast component of the ROSL decay curves for samples bal2 and kst4, as a function of the prior IR stimulation time. These curves are analyzed with Eq. (3).

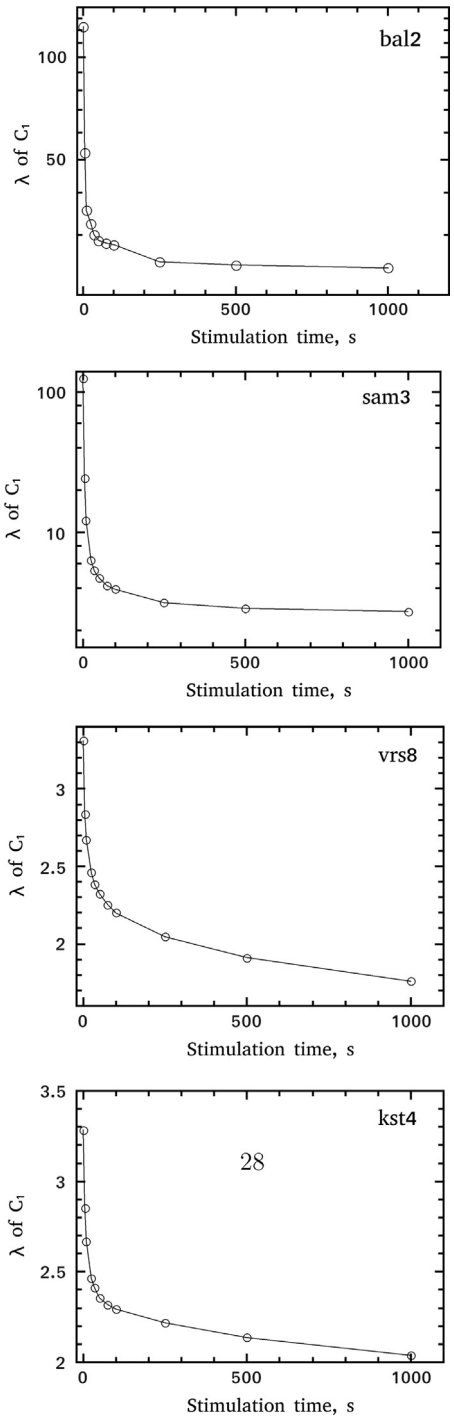

Fig. 7. The values of the decay constants λ of component C_1 of the ROSL decay curves of all feldspar samples, as a function of the prior IR stimulation time.

Table 2
Values of the parameter ρ' from the fitting of the CW-OSL decay curves using Eq. (3).

Sample	λ_1 (s^{-1})	ρ'_1	λ_2 (s^{-1})	ρ'_2
bal2	Fig. 7	$5.0 \times 10^{-4} \pm 1 \times 10^{-4}$	0.018 ± 0.001	$1.3 \times 10^{-5} \pm 1.1 \times 10^{-5}$
sam3	Fig. 7	$2.1 \times 10^{-4} \pm 1 \times 10^{-4}$	0.021 ± 0.006	$7.0 \times 10^{-5} \pm 1.9 \times 10^{-5}$
vrs8	Fig. 7	$4.4 \times 10^{-3} \pm 3 \times 10^{-4}$	0.004 ± 0.0002	$1.0 \times 10^{-2} \pm 3.1 \times 10^{-4}$
kst4	Fig. 7	$5.0 \times 10^{-3} \pm 1.5 \times 10^{-4}$	0.003 ± 0.0003	$9.0 \times 10^{-2} \pm 9.1 \times 10^{-3}$

using a feldspar sample which underwent an infrared bleaching process, followed by measurement of the CW-OSL signal.

The main Equation in Pagonis et al. [21] is again similar to Eq. (3), but with the functions $F(t)$ and $f(t)$ given by

$$F(t) = \ln(zA(T+t)) \tag{10}$$

$$f(t) = T + t \tag{11}$$

where T is an experimentally determined time shift factor.

5. Results and discussion

5.1. CCRA analysis of the ROSL signals based on the Lambert function

To the best of our knowledge Eq. (1) is applied for the first time in the OSL literature to analyze an extended series of experimental ROSL decay curves.

The goodness of fit in all component resolved analysis which will be presented below was tested by the Figure Of Merit (FOM) of Balian and Eddy [22].

Examples of component resolved ROSL decay curves using Eq. (1) are shown in Fig. 3 for samples bal2 and kst4. The behavior of feldspar sample sam3 was found to be exactly the same as for sample bal2, whereas the behavior of the vrs8 sample was very similar to that of sample kst4. In all cases analyzed, it was found that a minimum of three components were necessary in order to obtain a good fit, with FOM values between 0.8% and 1%. Using two components (not shown), the FOM values are increased to 5% and above, whereas using four components the FOM drops to 0.5%. This feature verifies the multi-component structure of the OSL signal already noticed by a simple observation of the LM-OSL in Fig. 2.

The mean values from the analysis of the decay constants λ and of the parameter $R = A_n/A_m$ of each component and for all experimental ROSL curves, are shown in Table 1. In our description we use the commonly used terminology of fast, medium and slow component for these three components.

The values of the parameter R indicate that the fast components correspond to a kinetic order $b \sim 1.4$, the medium components to $b \sim 1.6$ and the slow components to $b \sim 1.8$. It is concluded that within the estimated error of R, the kinetic order of each component is the same for all feldspar samples. It is noted that both the general order kinetic equation and Eq. (1) are based on the OTOR model, in which the kinetic order is related only to the ratio of the retrapping and recombination probabilities R. In more advanced models containing additional energy levels, the kinetic order is also affected by competition effects [23].

Although a high quality fit in the ROSL analysis was achieved using three components, it was not possible to isolate accurately the individual behavior of the fast and medium components, because of the many possible combinations which can give the same good fitting results. Therefore, Fig. 4 shows the behavior of the integrated sum of the fast and medium components as a function of the prior IRSL.

The integrated signal of the slow component resulting from the above analysis was found to be stable for all (eleven) prior IR stimulation times. The standard deviation from their mean values are 1.2%, 2.3%, 5.6% and 7% for bal2, sam3, vts8 and kst4 samples respectively.

From the above, it is clear that the IR stimulation can influence the fast component and does not influence significantly neither the medium nor the slow component. It is then concluded that IR stimulation most likely influences only the electron traps which are responsible for the fast component.

5.2. Tunneling analysis of the R-OSL curves

5.2.1. Analysis using Eq. (3)

Using Eq. (3), it was found that two tunneling components are required in order to fit the ROSL curves, instead of the three components necessary when using Eq. (1). Fig. 5 shows examples of component resolved ROSL decay curves using Eq. (3), for samples bal2 and kst4. Sample sam3 behaved exactly the same way as sample bal2, whereas sample vrs8 behaved the same as sample kst4. Furthermore, the FOM values obtained are of the order of 0.5% for all experimental ROSL decay curves and for all feldspar samples. These FOM values are obviously better than the FOM values between 0.8 and 1% obtained using Eq. (1) in Section 4.1. The successful fitting of the ROSL decay curves using the analytical tunneling expression from a localized transition model was rather surprising.

Fig. 6 shows the behavior of the integrated signal of the first component as a function of the prior IR stimulation time. The integrated signal of the second tunneling component in the ROSL curves was found to be stable for all prior IR stimulation times, as discussed above.

The above analysis on integrated signals verifies the conclusion in the previous Section 5.1 that the IR stimulation influences only the electron traps that are responsible for the fast component.

The parameters obtained from fitting the ROSL curves are the dimensionless carrier density ρ' and the decay constant λ (which is proportional to the optical stimulation cross section). The values of ρ' did not follow a systematic behavior as a function of the prior IR stimulation time, and therefore only their mean values are

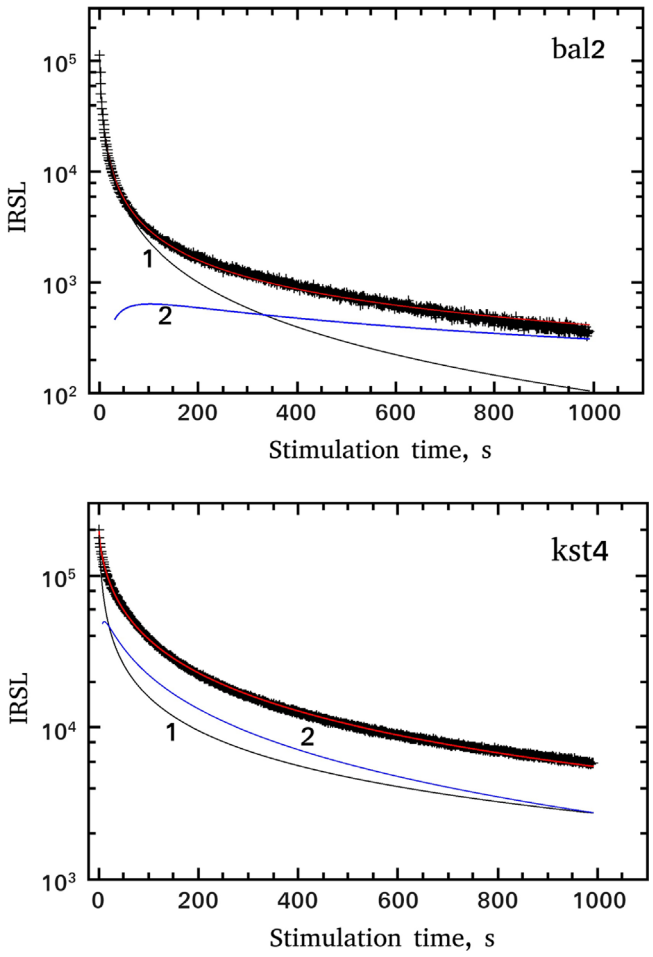

Fig. 8. CW-IRSL decay curves for samples bal2 and kst4, analyzed using Eq. (3).

Table 3
Mean values of the parameters ρ' and λ (in s^{-1}) from the fitting of the CW-IRSL decay curves using Eq. (3). The mean values were evaluated from the CW-IRSL for stimulation times above 75 s.

Sample	ρ'_1	λ_1 (s^{-1})	ρ'_2	λ_2 (s^{-1})
bal2	$3.3\times10^{-3}\pm5\times10^{-4}$	10.8 ± 0.9	$1.2\times10^{-4}\pm3\times10^{-5}$	0.03 ± 0.001
sam3	$4.0\times10^{-3}\pm3\times10^{-4}$	5.62 ± 0.3	$1.0\times10^{-3}\pm4\times10^{-5}$	0.03 ± 0.001
vrs8	$2.3\times10^{-4}\pm9\times10^{-5}$	5.23 ± 0.5	$3.3\times10^{-3}\pm5\times10^{-4}$	0.83 ± 0.040
kst4	$2.5\times10^{-4}\pm1\times10^{-4}$	5.5 ± 0.3	$2.0\times10^{-3}\pm1\times10^{-3}$	0.21 ± 0.001

listed in Table 2. The most general conclusion is that the ρ' values for the sanidine samples (bal2 and sam3) are lower than the ρ' values of vrs8 (orthoclase) and kst4 (microcline). This difference was not obtained for these samples in the results of Sfampa et al. [11], where, however, the pre-conditioning of bleaching by blue light was much stronger than the bleaching by IR in the present work.

The values of the decay constant λ show a very interesting variation as a function of the prior IRSL time, so they are given for all feldspar samples in Fig. 7. The general observation is that the λ value drops sharply from 0 s of IR stimulation time up to 100 s of stimulation time. Furthermore, the feldspar samples bal2 and sam3 (both sanidine) show very high values of λ between 0 s and 100 s of prior IR stimulation times, whereas the other two samples i.e. vrs8 (orthoclase) and kst4 (microcline) have much smaller values of λ.

Concerning the second component its value of decay constant, listed in Table 2, was stable after all the IR stimulation times. This result is attributed to the fact that the IRSL has not influenced electron traps responsible for the slow OSL component. Therefore, the behavior of the decay constants shown in Fig. 7 and listed in Table 2 verifies again the conclusion that the IRSL influences only the electron traps responsible for the fast OSL component.

The presence of two components in the tunneling analysis is consistent with the recent work by Sfampa et al. [11]. These authors carried out a detailed study of the IRSL signals from ten natural K-feldspar which included sanidine, orthoclase and microcline samples. The CW-IRSL curves from these ten samples were fitted using analytical tunneling equations and two tunneling components were found, which are presumed to originate from two different energy levels undergoing tunneling recombination. These two components were termed “fast” and “slow”, and the corresponding stimulation cross sections for the sanidine feldspars were found to be very different from those of the orthoclase and microcline feldspars.

5.2.2. Analysis using Eqs. (7) and (10)

All CW-OSL curves are fitted successfully using Eqs. (7) and (10) (FOM better than 1%). However, more important than the good fits is the interpretation of the fitting parameters. The general Eq. (3) becomes a four-parameter equation when Eqs. (7) and (10) are used. The fourth parameter is the time shift τ_0 for Eq. (7), and the time shift T for Eq. (10).

Unfortunately, the experimental value of the time shift for Eq. (7) is $1<\tau_0<10$ s, which is very small compared with the values reported by Jain et al. [20]. As a consequence of these small τ_0 and T values, it was not possible to discriminate these small shifts. Nevertheless, our attempts to fit the experimental data using these equations gave some useful results, which are listed below.

- Case I: The parameters τ_0 and T were left free during the fitting process. In these cases the time shifts τ_0 and T cannot be determined accurately, because very good fits can be obtained for many pairs of the free parameters J and τ_0.
- Case II. The free parameter τ_0 was fixed to its experimental value of less than 10 s. In this case very good fits were also obtained. In addition, the resulting values of the free fitting parameters ρ' are similar to the values of ρ' obtained from using Eq. (3) . These best fitting values are given in Table 2. The resulting best fitting values of the free parameter J follow the same trends as the parameter λ in Fig. 7. However, these values of J are far from the value of 10^{-5} reported by Jain et al. [20]. It must be noted, however, that these values should be comparable with values of Jain et al. [20] if $b=s$, i.e. or when the attempt-to-tunneling factor b is equal to attempt-to-escape factor s.

In both the works of Jain et al. [20] and Pagonis et al. [21], the decay curves are analyzed by using only one tunneling component. Therefore, it was decided to attempt fitting the data with a single component, using Eqs. (7) and (10). The one component fits were very inaccurate for samples bal2 and sam3, and questionable for the case of sample vrs8. On other hand, such a single component fit was quite successful for the kst4 feldspar. This is due to the low intensity of the second component in this sample, as it seen in Fig. 5.

5.3. Tunneling analysis of IRSL signals

The CW-IRSL curves measured in step 2 of the experimental protocol were also subjected to component resolved analysis using only the tunneling Eq. (3), because these measurements are received just after the irradiation without any pre-conditioning. Examples of component resolved IRSL decay curves are shown in Fig. 8 for samples bal2 and kst4. The results for sample sam3 were similar to those for bal2 and the results for vrs8 feldspar were again similar to those for sample kst4. A basic difference is that in the sanidine samples bal2 and sam3 the second component is relatively insignificant, whereas for vrs8 (orthoclase) and kst4 (microcline) both components are significant. The fitting parameters λ and ρ' are listed in Table 3. The general conclusion from this table is that the ρ' values of the second component are greater than the values of the first component. This result is in agreement with the corresponding results by Sfampa et al. [11].

6. Conclusions

1. The newly developed Eq. (1) for delocalized transitions gave excellent fits to all ROSL decay curves. Three components were necessary in order to achieve good fits to all data.
2. Eq. (3) which is derived from a localized transition model, fits very successfully the ROSL decay curves. In fact it gives better fits than the delocalized model Eq. (1), and requires only two components. This is a new finding, since all component resolved analysis of ROSL decay curves existing in literature are attempted using the empirical general order kinetics equation, which is based on delocalized models.

3. Experimental IRSL curves are also fitted successfully with the tunneling Eq. (3), which is derived from a localized tunneling model.
4. The prior IR stimulation of the feldspar samples was found to influence the initial part of ROSL curve, which corresponds to the fast ROSL components.
5. The electron trapping levels responsible for the IRSL emission may also be responsible for the fast ROSL components.

References

[1] A.G. Wintle, J. Lumin. 15 (1977) 385.
[2] R. Visocekas, T. Ceva, C. Marti, F. Lafaucheux, M.C. Roberts, Phys. Status Solidi A 35 (1976) 315.
[3] D.J. Huntley, J. Phys.: Condens. Matter 18 (2006) 1359.
[4] E. Bulur, Radiat. Meas. 26 (1996) 701.
[5] G. Kitis, C. Furetta, V. Pagonis, Mod. Phys. Lett. B 23 (2009) 3191.
[6] G. Kitis, N.D. Vlachos, Radiat. Meas. 48 (2013) 47.
[7] G. Kitis, V. Pagonis, J. Lumin. 137 (2013) 109.
[8] M. Jain, C. Ankjærgaard, Radiat. Meas. 46 (2011) 292.
[9] M. Jain, B. Guralnik, M.T. Andersen, J. Phys.: Condens. Matter 24 (2012) 385402.
[10] G.S. Polymeris, E. Thodosoglou, G. Kitis, N.C. Tsirliganis, A. Koroneos, K.M. Paraskevopoulos, Mediter. Archeol. Archeom. 13 (2013) 155–161.
[11] I.K. Sfampa, G.S. Polymeris, V. Pagonis, E. Theodosoglou, N.C. Tsirliganis, G. Kitis, Nucl. Instrum. Methods Phys. Res. B 359 (2015) 89.
[12] R.M. Corless, G.H. Gonnet, D.G.E. Hare, D.J. Jeffrey, D.E. Knuth, On the lambert W function, Adv. Comput. Math. 5 (1996) 329–359.
[13] A.M. Sadek, H.M. Eissa, A.M. Basha, G. Kitis, J. Lumin. (2014).
[14] A.M. Sadek, H.M. Eissa, A.M. Basha, G. Kitis, Nucl. Instrum. Methods Phys. Res. B 330 (2014) 103.
[15] A.M. Sadek, H.M. Eissa, A.M. Basha, E. Carinou, P. Askounis, G. Kitis, Appl. Radiat. Isot. 95 (2015) 214.
[16] A.M. Sadek, H.M. Eissa, A.M. Basha, G. Kitis, Phys. Status Solidi B 252 (2015) 721.
[17] ROOT, A Data Analysis Framework, ⟨https://root.cern.ch⟩.
[18] MINUIT, A Physics Analysis Tool for Function Minimization, Released in ROOT.
[19] GSL-GNU Scientific Library, ⟨http://www.gnu.org/software/gsl⟩.
[20] M. Jain, R. Sohbati, B. Guralnik, A.S. Murray, M. Kodok, T. Lapp, A.K. Prasad, K. J. Thomsen, J.P. Buylaert, Radiat. Meas. (2015), http://dx.doi.org/10.1016/j.radmeas.2015.0.2.006.
[21] V. Pagonis, G. Polymeris, G. Kitis, Radiat. Meas. (2015), http://dx.doi.org/10.1016/j.radmeas.2015.09.002.
[22] Balian, Eddy, Nucl. Instrum. Methods 145 (1977) 389.
[23] V. Pagonis, G. Kitis, Phys. Status Solidi B 249 (2012) 1590.